

# Analog sensitive chemical inhibition of the DEAD-box protein DDX3

Stephen N. Floor,<sup>1,2</sup> Krister J. Barkovich,<sup>3</sup> Kendall J. Condon,<sup>1</sup>  
 Kevan M. Shokat,<sup>3,4,5\*</sup> and Jennifer A. Doudna<sup>1,2,5,6,7\*</sup>

<sup>1</sup>Department of Molecular and Cell Biology, University of California, Berkeley, California

<sup>2</sup>Howard Hughes Medical Institute, University of California, Berkeley, Berkeley, California

<sup>3</sup>Department of Cellular and Molecular Pharmacology, University of California, San Francisco, California

<sup>4</sup>Howard Hughes Medical Institute, University of California, San Francisco, California

<sup>5</sup>Department of Chemistry, University of California, Berkeley, California

<sup>6</sup>Innovative Genomics Initiative, University of California, Berkeley, Berkeley, California

<sup>7</sup>Lawrence Berkeley National Laboratory, Physical Biosciences Division, Berkeley, California

Received 23 October 2015; Accepted 1 December 2015

DOI: 10.1002/pro.2857

Published online 10 December 2015 proteinscience.org

**Abstract:** Proper maintenance of RNA structure and dynamics is essential to maintain cellular health. Multiple families of RNA chaperones exist in cells to modulate RNA structure, RNA–protein complexes, and RNA granules. The largest of these families is the DEAD-box proteins, named after their catalytic Asp–Glu–Ala–Asp motif. The human DEAD-box protein DDX3 is implicated in diverse biological processes including translation initiation and is mutated in numerous cancers. Like many DEAD-box proteins, DDX3 is essential to cellular health and exhibits dosage sensitivity, such that both decreases and increases in protein levels can be lethal. Therefore, chemical inhibition would be an ideal tool to probe the function of DDX3. However, most DEAD-box protein active sites are extremely similar, complicating the design of specific inhibitors. Here, we show that a chemical genetic approach best characterized in protein kinases, known as analog-sensitive chemical inhibition, is viable for DDX3 and possibly other DEAD-box proteins. We present an expanded active-site mutant that is tolerated *in vitro* and *in vivo*, and is sensitive to chemical inhibition by a novel bulky inhibitor. Our results highlight a course towards analog sensitive chemical inhibition of DDX3 and potentially the entire DEAD-box protein family.

**Keywords:** chemical genetics; DEAD-box proteins; small-molecule inhibitor; RNA; protein engineering; DDX3 inhibitor

*Abbreviations:* AMP, adenosine monophosphate; hnRNP, heteronuclear ribonucleoprotein

Additional Supporting Information may be found in the online version of this article.

Stephen N. Floor and Krister J. Barkovich contributed equally to this work.

\*Correspondence to: Jennifer A. Doudna, University of California, Berkeley, 708A Stanley Hall, Berkeley, CA 94720. E-mail: doudna@berkeley.edu and Kevan M. Shokat, University of California, San Francisco, 600 16th St MC 2280, San Francisco, CA 94158. E-mail: kevan.shokat@ucsf.edu

## Introduction

RNA is a highly dynamic macromolecule and can form numerous intra- and inter-molecular structures, which influence function. Like proteins, RNA molecules have chaperones that remodel structures to ensure proper function. RNA chaperones can be ATP-dependent like DEAD-box proteins,<sup>1</sup> or ATP-independent like cold shock domain proteins and heteronuclear ribonucleoproteins (hnRNPs).<sup>2</sup> In humans, there are 36 DEAD-box proteins which function in every step of RNA biology. For example, 18 DEAD-box proteins have been implicated in

ribosome assembly, six in splicing, six in translation, and others in numerous other functions.<sup>1</sup> DEAD-box proteins also associate with non-membrane-bound, microscopically visible puncta in cells known as RNA granules,<sup>3,4</sup> which are thought to arise from phase separation caused by multivalent weak interactions.<sup>5–7</sup> Remarkably, loss of function of the *C. elegans* DEAD-box protein CGH-1 (human DDX6) causes germ line granules to form square, crystalline structures *in vivo*.<sup>8</sup> Therefore, DEAD-box proteins can function both on individual RNA:protein complexes (RNPs), or function as molecular dispersants to promote fluidity of RNA granules.

The human DEAD-box protein DDX3 (encoded by *DDX3X*) and its yeast ortholog *DED1* have been implicated in numerous cellular functions, but most consistently in remodeling RNA and RNPs during translation initiation.<sup>4,9–13</sup> DDX3 and Ded1p also associate with two related types of RNA granules known as stress granules and P-bodies,<sup>3,4</sup> and introduction of catalytically deficient Ded1p increases granule size,<sup>4</sup> suggesting they may have a role in determining the size of RNA granules by modulating weak interactions. Frequent mutations of *DDX3X* are found in numerous human malignancies including medulloblastoma,<sup>14–17</sup> diverse blood cancers,<sup>18–21</sup> head and neck squamous cell carcinoma,<sup>22,23</sup> lung cancer,<sup>24</sup> and more. However, cellular studies are complicated by the fact that DDX3 and *DED1* are essential genes, limiting the perturbations that can be made. Moreover, the poor time resolution of knockdown and transfection experiments complicates assignment of direct and indirect targets of DDX3 in cells.

DDX3, like all DEAD-box proteins, couples ATP binding to conformational changes that create a binding surface selective for single stranded RNA.<sup>1,25</sup> ATP hydrolysis then destabilizes this conformation and promotes product release.<sup>26</sup> Conversion to the ATP-bound closed state involves creation of a composite active site involving residues on both the N-terminal DEAD and C-terminal HELICc domains. Therefore, interfering with ATP binding or hydrolysis will prevent RNA and RNP remodeling by DEAD-box proteins.

Chemical inhibitors are extremely powerful tools to study function in cells due to their high temporal resolution. However, it is difficult to develop specific inhibitors to protein families with many highly related members, like DEAD-box proteins. In protein kinases, mutation of a “gatekeeper” residue to a smaller alanine or glycine uniquely sensitizes the mutant protein to bulky active site inhibitors which are otherwise inactive against the majority of the kinome.<sup>27</sup> This approach allows for high affinity and specific inhibition of individual protein kinases by introducing a single point mutation, and has been widely used to generate analog sensitive

inhibitors<sup>27</sup> and artificial substrates.<sup>28</sup> A similar approach has been used to generate synthetic substrates or inhibitors for myosin and kinesin.<sup>29,30</sup>

Here, we present proof-of-principle experiments demonstrating analog sensitive inhibition of the DEAD-box protein DDX3. We engineer a binding pocket near the ATP binding site by point mutation while retaining *in vitro* function and complementation of the essential yeast gene *DED1*. The expanded active-site mutant is sensitized to pyrazolopyrimidine-related compounds *in vitro*, including GXJ1-76. In yeast, treatment with GXJ1-76 is lethal in cells harboring expanded active-site mutants, but this is due to synthetic interactions with temperature sensitivity rather than specific inhibition. We therefore performed a general screen of existing analog-sensitive inhibitors and find a new series of compounds that also demonstrate more potent analog sensitive inhibition *in vitro*. Taken together, our results demonstrate that analog sensitive inhibition of DEAD-box proteins is possible, and highlight two scaffolds that could be used to design high affinity inhibitors.

## Results

### Targeting a hydrophobic cluster for expanded active-site mutation

Analog sensitive inhibition of proteins requires generation of an expanded active-site to accommodate bulky groups on the inhibitor. We examined the ATP binding site of DDX3 and found that the N6 position of adenosine points towards a cluster of four hydrophobic residues on the DEAD domain [Fig. 1(A)].<sup>31</sup> As N6 on adenosine is the position modified in many preexisting bulky kinase inhibitors and adenosine receptor agonists, we targeted this hydrophobic cluster for mutation. We then examined the conservation of this region in diverse human DEAD-box proteins and found high conservation at most positions but some variability [Fig. 1(B)]. Expanding this analysis to DEAD-box proteins from *Saccharomyces cerevisiae* and *Escherichia coli* shows that all four positions are tolerant of substitutions, suggesting some structural plasticity in this region [Fig. 1(C)]. Therefore, there is a hydrophobic cluster adjacent to the ATP binding site that is conserved but also shows limited variability, suggesting it may be tolerant to mutation.

### Expanded active-site mutants of DDX3 are functional

We generated point mutants of three positions of the hydrophobic cluster in DDX3 [Fig. 1(A)] and expressed and purified them from *E. coli*. All three variants eluted from a gel filtration column normally, suggesting no major disturbance in folding [Fig. 2(A)]. We used a shortened construct of DDX3

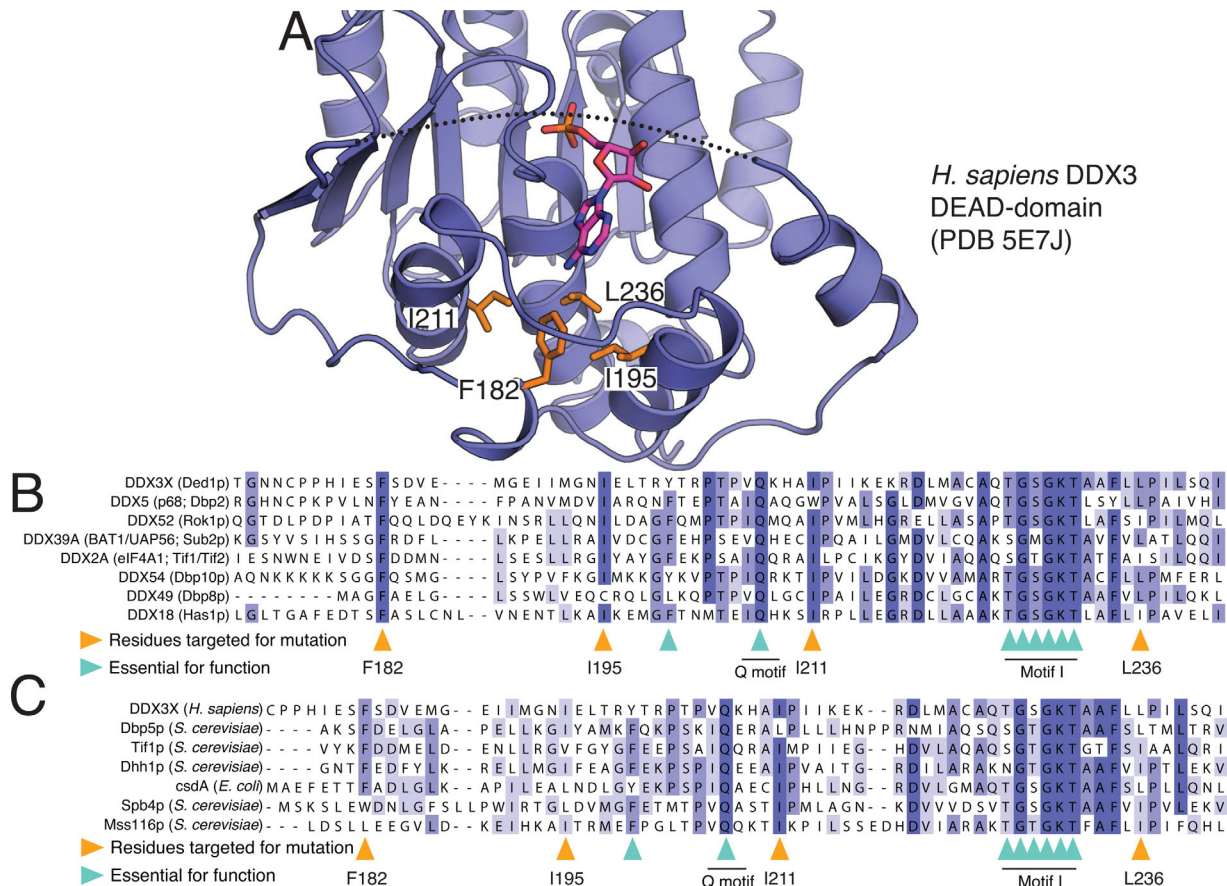


**Figure 1.** Targeting a hydrophobic cluster adjacent to the ATP binding pocket of DDX3 for mutation. (A) A structural view of the ATP binding pocket in human DDX3 bound to AMP (PDB 5E7J). AMP is in purple, DDX3 is in blue, the hydrophobic cluster residues are in orange, and a disordered region not visible in the structure is represented by a dotted black line. (B,C) Sequence alignments of eight human DEAD-box proteins (B) or seven DEAD-box proteins from various organisms (C) showing overall conservation but some plasticity of the hydrophobic cluster residues. Core conserved motifs of DEAD-box proteins are indicated.

lacking the N- and C-terminal tails that has superior biochemical behavior and is highly active *in vitro* (DDX3 residues 132-607).<sup>31</sup> As F182 abuts the ATP binding pocket, we tested the ability of the mutant protein to bind to the nucleotide adenosine monophosphate (AMP). We used AMP rather than ATP to directly test the binding affinity of nucleotide to the DEAD domain without avidity effects from the HELICc domain caused by ATP-dependent conformational changes.<sup>1</sup> Both wild-type and the most severe mutation, F182A, have similar affinity to AMP [Fig. 2(B)],<sup>32</sup> indicating that nucleotide binding is not affected by this mutation. The observation that the I195A and I211A point mutants exhibit less severe defects in duplex unwinding than F182A [Fig. 2(C)] and yeast growth [Fig. 2(D)] suggests that they also bind nucleotide with similar affinity to wild-type DDX3, but we have not tested this directly.

We next functionally characterized the mutant proteins with expanded active sites. First, we tested the activity of the mutant proteins in RNA duplex unwinding assays<sup>33</sup> and found that all mutants had

reduced activity to varying degrees [Fig. 2(C)]. As a further test, we determined the ability of the mutant alleles to complement the essential yeast gene *DED1* *in vivo*, and found that all three alleles are sufficient for growth at normal temperature, despite the *in vitro* defects [Fig. 2(D)]. However, the I157A (DDX3 I195A) and F144A (F182A) variants exhibit cold and heat sensitivity, respectively [Fig. 2(D)]. It is surprising that these mutations are tolerated in yeast given their large kinetic defects *in vitro* [Fig. 2(C)]. It is possible that the effect of the mutations on Ded1 is not the same as that on DDX3, or that the yeast gene *DBP1*, which is a high-copy suppressor of *DED1*,<sup>34</sup> is compensating for partially functional Ded1p. In sum, mutation of the active-site hydrophobic cluster is tolerated *in vitro* and *in vivo*, demonstrating it is possible to create an expanded active site in a DEAD-box protein.

#### **Adenosine monophosphate but not published DDX3 inhibitors retards RNA duplex unwinding**

We started to search for a viable scaffold for engineering bulky active-site inhibitors of DDX3 by

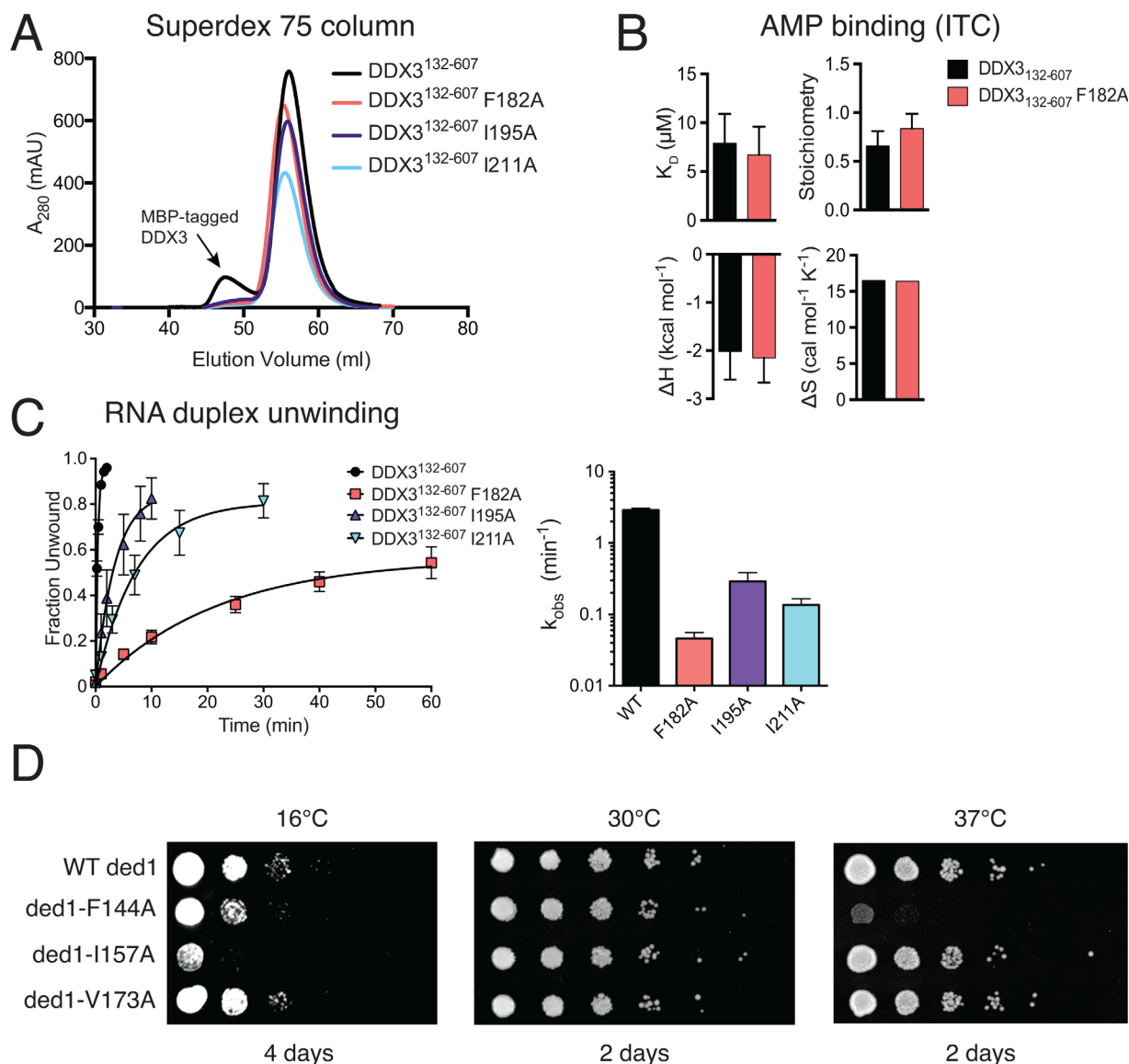


**Figure 2.** Hydrophobic cluster mutants of DDX3 support function *in vitro* and *in vivo*. (A) The indicated mutants of DDX3 purify normally as shown by their elution from a Superdex 75 gel filtration column. The indicated smaller peak to the left is uncleaved protein attached to the His-MBP tag. (B) DDX3<sup>132-607</sup> wild-type and F182A bind AMP identically based on isothermal titration calorimetry. Error is standard error of the fit parameter. (C) The hydrophobic cluster mutants are able to unwind RNA duplexes *in vitro* but at slower rates than wild-type DDX3<sup>132-607</sup>. Error is S.D (left) and standard error of the fit parameter (right). (D) Yeast with hydrophobic cluster mutants in the sole copy of *DED1* grow normally at 30°C but some exhibit cold (I157A) or heat (F144A) sensitivity. Yeast *DED1* F144, I157, and V173 correspond to DDX3 F182, I195 and I211, respectively. Spots represent a tenfold dilution series from OD 1.

surveying published inhibitors. To verify that our duplex unwinding assay was able to measure inhibition of DDX3 we titrated AMP into the reaction, which binds with low micromolar affinity [Fig. 2(B)] and inhibits the enzyme.<sup>32</sup> We observed endpoint depression of duplex unwinding with only a two-fold effect on the rate with an apparent  $K_I$  of  $\sim 30 \mu M$  [Fig. 3(A,B)]. We then tested a series of published inhibitors including one rhodanine derivative,<sup>35</sup> two triazine derivatives,<sup>35</sup> the ring-expanded nucleoside RK-33,<sup>24</sup> ketorolac salt,<sup>36</sup> and kaempferol-3-O-b-D-glucopyranoside.<sup>37</sup> Both ketorolac salt and Maga

compound 4b showed two-fold effects on the rate of duplex unwinding but no change to the endpoint of the reaction [Fig. 3(C,D)]. As ATP hydrolysis is required for product release but not duplex unwinding,<sup>26</sup> it is possible that endpoint depression [Fig. 3(B)] is a signature of active-site inhibition while rate depression reflects noncompetitive inhibition by, for example, interacting with the duplex RNA substrate [Fig. 3(D)]. Alternatively, as Ded1p exhibits both ATP-dependent duplex unwinding and ATP-independent strand annealing activities,<sup>38</sup> it may be that ATP-competitive inhibition causes endpoint

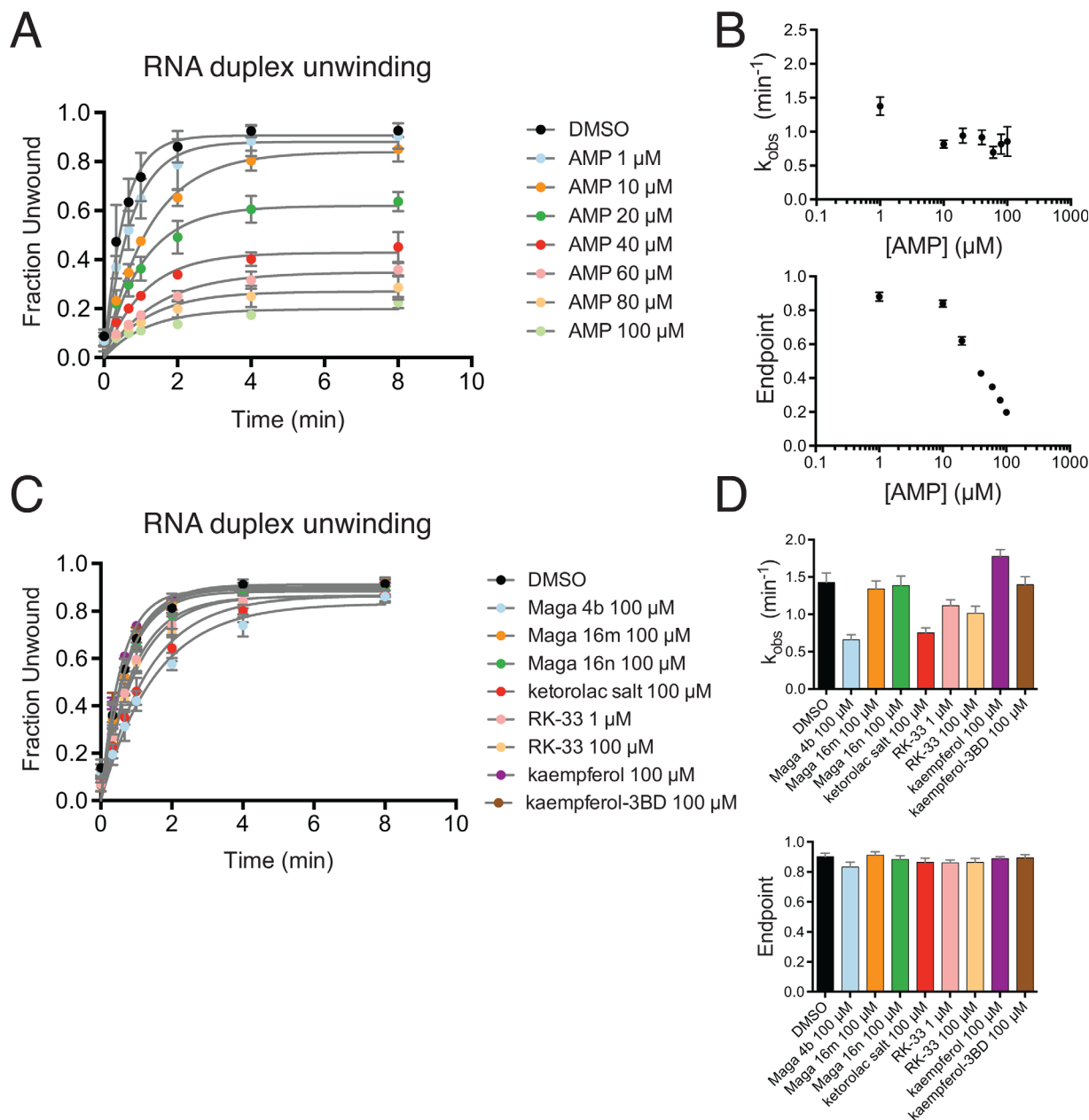


**Figure 3.** Adenosine monophosphate, but not putative DDX3 inhibitors, retards duplex unwinding *in vitro*. (A,B) RNA duplex unwinding with AMP exerts concentration-dependent inhibition (A) and depresses the reaction endpoint but not rate (B). (C,D) Duplex unwinding with seven published inhibitors of DDX3 (C) and fitted parameters (D) does not change the reaction endpoint and decreases the rate by at most two-fold. (A,C) Error is S.D.; (B,D) standard error of the fit parameter.

depression by altering the balance between unwinding and annealing. It remains possible that these inhibitors interact with the noncatalytic extensions that have been removed from DDX3<sup>132-607</sup>, or that they interact with a composite bimolecular surface that only exists in cells. As we were unable to observe strong inhibition with any of the tested compounds other than AMP, we sought alternatives to screen for analog sensitive inhibitors of DDX3.

#### Analog sensitive inhibition of DDX3

We surveyed diverse compounds in an attempt to find analog sensitive inhibitors of our expanded

active site versions of DDX3. Focus was placed on the F182A mutation as it generates the largest pocket for a bulky inhibitor. We assembled a panel of nine adenosine receptor agonists, three AAA<sup>+</sup>-ATPase inhibitors or related quinazolinones,<sup>39</sup> and ~30 bulky kinase inhibitors and tested these using duplex unwinding. Kinase inhibitors were included because these have been shown to exhibit cross-reactivity with DEAD-box proteins.<sup>40,41</sup> We found no inhibitory activity of any of the adenosine receptor analogs and weak activity for the AAA<sup>+</sup>-ATPase DBeQ (data not shown). In addition, the large majority of the kinase inhibitors tested showed no

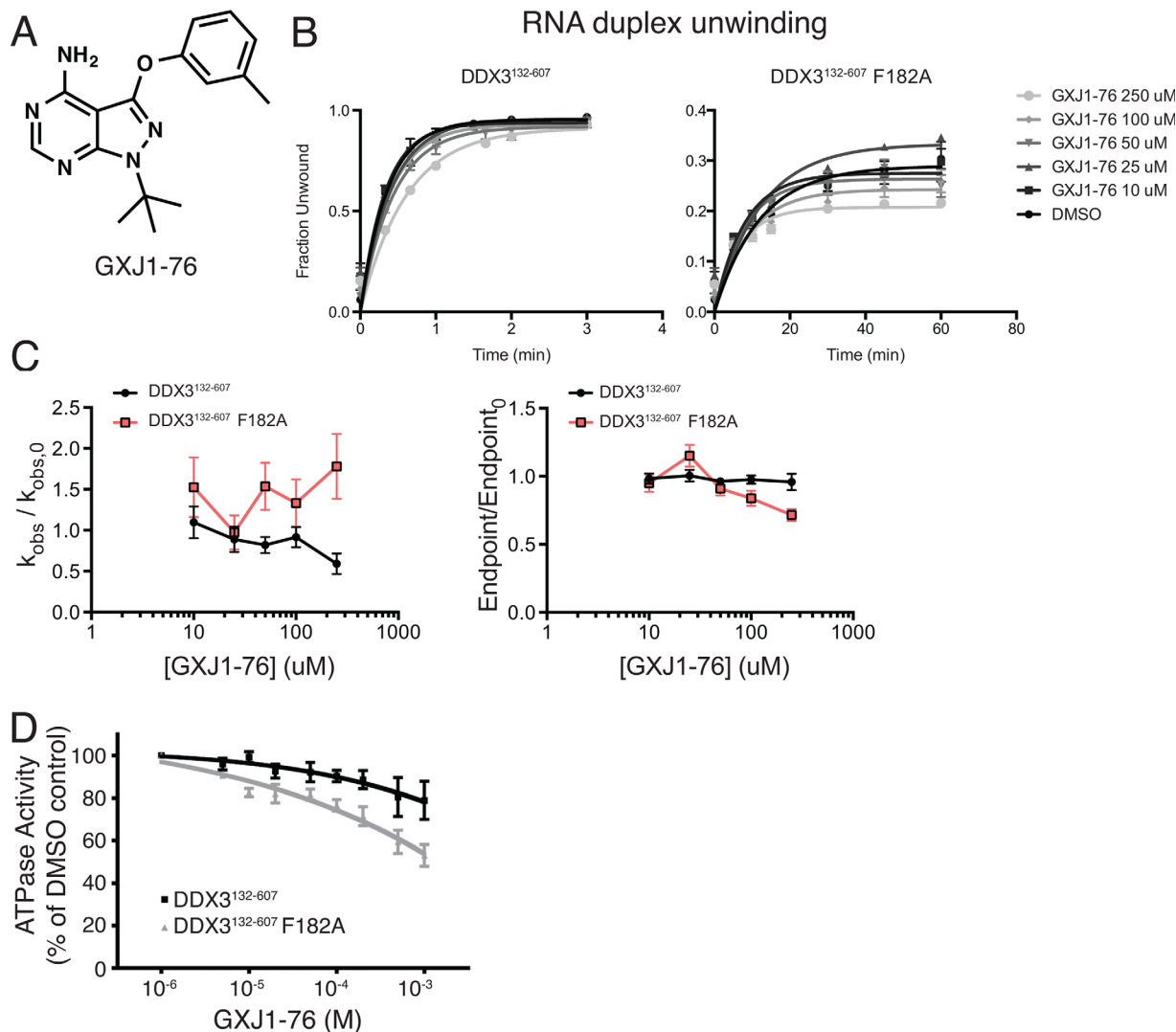


**Figure 4.** Analog sensitive inhibition of DDX3. (A) The structure of the initial lead compound GXJ1-76, which is a pyrazolopyrimidine-based inhibitor. (B) Treatment of wild-type DDX3<sup>132-607</sup> with GXJ1-76 does not affect duplex unwinding (left), but treatment of DDX3<sup>132-607</sup> F182A causes a reduction in the duplex unwinding endpoint in a concentration dependent manner (right). Error is S.D. (C) The relative unwinding rate and endpoint compared to the rate and endpoint with no compound as a function of GXJ1-76 concentration. Error is propagated error of the fit parameter. (D) GXJ1-76 shows modest selectivity towards DDX3<sup>132-607</sup> F182A in ATP hydrolysis. Error is S.D.

effect. However, we found reproducible inhibition of duplex unwinding of only the mutant allele upon addition of the compound GXJ1-76 [Fig. 4(A,B)]. The concentration dependence of GXJ1-76 treatment is not linear [Fig. 4(B)], possibly due to solubility issues at these concentrations. Notably, GXJ1-76 causes endpoint depression with only small changes on the rate [Fig. 4(C)] as seen for AMP [Fig. 3(A,B)], suggesting it is targeting the active site. GXJ1-76 shows a dose-dependent decrease in the ATPase activity of DDX3 with modest selectivity for the mutant allele [Fig. 4(D)].

We then tested the ability of GXJ1-76 to inhibit Ded1p in yeast where the sole copy of *DED1* has been replaced by the expanded active-site allele F144A (DDX3 F182A; Figure 2(D)). Yeast harboring

a wild-type allele of *DED1* are minimally affected by treatment with 100  $\mu$ M GXJ1-76 but *ded1*-F144A yeast grow considerably slower in the presence of GXJ1-76 [Fig. 5(A)] As the *ded1*-F144A strain exhibits temperature sensitivity, we also tested inhibition in an unrelated temperature sensitive strain harboring mutations in the *MCM3* replicative helicase<sup>42</sup> to ensure that the growth defect was specific to GXJ1-76 interacting with Ded1p [Fig. 5(B)]. However, GXJ1-76 treatment also severely inhibited growth of the *mcm3-1* strain [Fig. 5(C)], suggesting that the growth inhibition observed is due to off-target effects. In sum, expanded active-site versions of DDX3 are preferentially inhibited by GXJ1-76 *in vitro*, but low potency and off-target effects in cells preclude use of this compound as is.

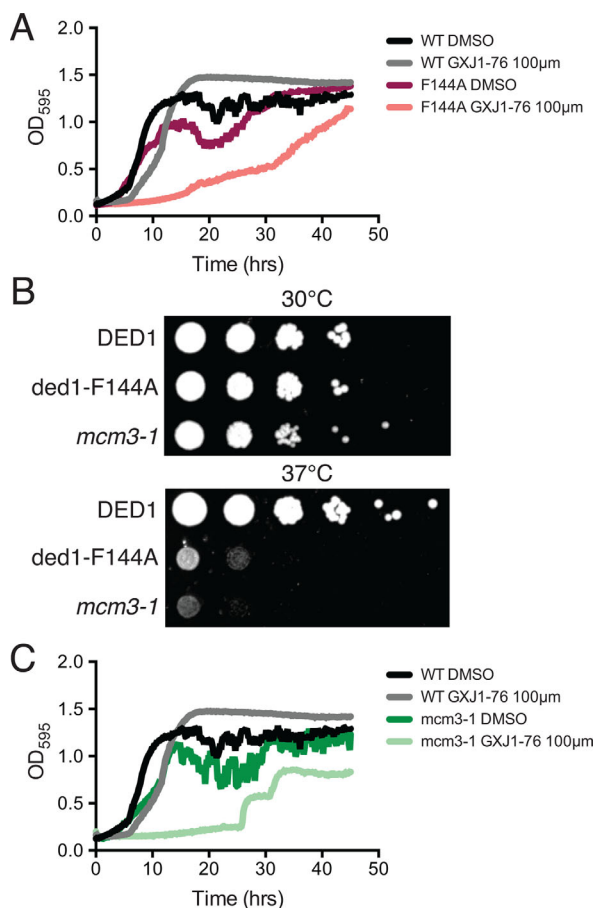


**Figure 5.** Expanded active-site alleles of *DED1* and other temperature sensitive yeast strains are inhibited by GXJ1-76. (A) A yeast strain harboring the expanded site allele *ded1-F144A* as the sole copy of *DED1* is inhibited by GXJ1-76. Continuous growth with OD<sub>595</sub> measurements is plotted. (B) Tenfold serial dilutions of *DED1*, *ded1-F144A* and *mcm3-1* yeast strains from OD 1 indicating similar growth at 30°C and temperature sensitivity at 37°C. (C) Growth of the *mcm3-1* strain is also inhibited by GXJ1-76, indicating that the results in (A) likely result from off-target effects.

### Bulky kinase inhibitor screen identifies anilinoquinazolines as lead scaffold

The biochemical inhibition of the mutant allele of DDX3 by GXJ1-76 (Fig. 4) suggests that kinase inhibitor scaffolds may provide a promising lead for the development of analog-sensitive DEAD-box helicase inhibitors. We therefore performed a more general screen of 31 bulky analog-sensitive kinase inhibitors (see Supporting Information Fig. S1). From this screen we hoped to identify a scaffold or bulky group that had increased potency against analog-sensitive mutants and retained selectivity over the wild-type allele. The screen included mostly pyrazolopyrimidine-based molecules with various substitutions at both the 3- and N1-positions. A number of the N1-substitutions had potential hydrogen bond donors or acceptors that we hoped might form favorable interactions within the binding

pocket to increase potency compared to GXJ1-76. The screen also included alternate inhibitor scaffolds beyond the pyrazolopyrimidine including pyrimidine-, and anilinoquinazoline-based inhibitors which we hoped would have different inherent affinity for the DEAD-box helicase ATP-binding site. From this screen, we identified AQZ01, a 6,7-dimethoxyanilinoquinazoline, as the most potent inhibitor of the F182A mutant (Fig. 6).

### Structure-activity relationship of AQZ01 yields compound 1, a selective analog-sensitive DEAD-box helicase inhibitor

Using screening hit AQZ01 as a starting point, we synthesized a series of molecules with increased steric bulk off the aniline of AQZ01 [Fig. 7(A)]. Interestingly, we found a strong preference for planar aromatic substitutions, as meta-bromo, isopropyl, or *tert*-butyl anilines exhibit little activity against the F182A mutant. The position of the planar fused aromatic ring is also important, as the 1-aminonaphthalene compound (AQZ04) was much more potent than the 2-aminonaphthalene compound (AQZ05). The most promising derivative of this series, AQZ06, contains a 4-aminoindole at this position and retained the selectivity of AQZ01 against wild-type DDX3, but increased potency against the F182A mutant substantially [Fig. 7(B)].

Assuming the 4-aminoindole of AQZ06 points into the pocket created by mutation of F182 of the hydrophobic cluster, we reasoned that changing the substitution of the 6- and 7-positions of AQZ06 could increase potency by making favorable interactions with the phosphate-binding P-loop of the helicase ATP-binding site. We therefore focused on placing hydrogen-bond donors/acceptors at the 6- and 7-positions of the anilinoquinazoline scaffold. Although we explored a series of molecules with formal

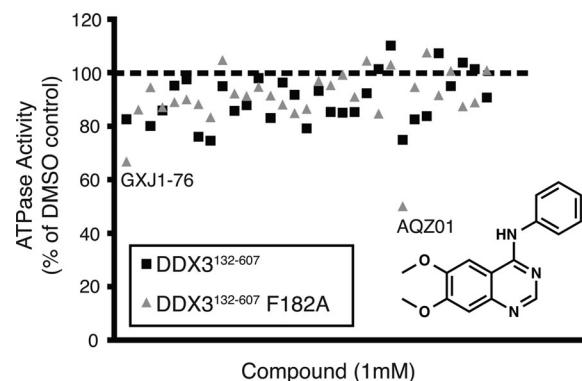


**Figure 6.** Screen for analog-sensitive DEAD-box helicase inhibitors identifies anilinoquinazoline scaffold. The activity of 31 existing analog-sensitive kinase inhibitors against wild-type and F182A DDX3<sup>132-607</sup> was screened by an ATPase assay at 1 mM concentration. The structure of AQZ01, the most promising lead from this screen, is shown.

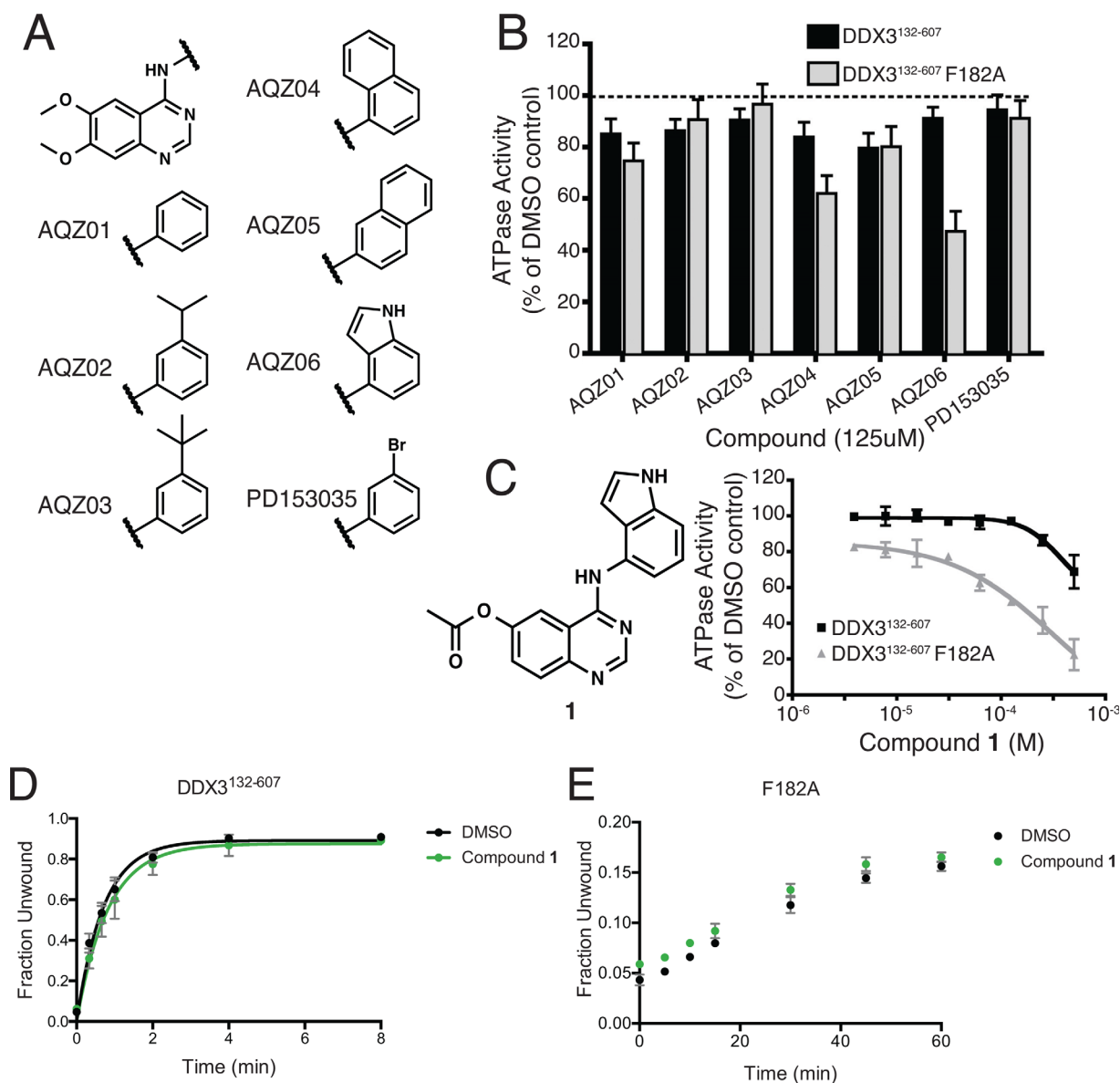


**Figure 7.** Chemical derivatization of AQZ01 yields compound **1**. (A) A series of molecules were synthesized to contain bulky groups off the aniline of AQZ01. (B) These analogs show stronger inhibition of DDX3<sup>132-607</sup> F182A by a 4-aminoindole (AQZ06) off the 6,7-dimethoxyanilinoquinazoline scaffold in an ATPase assay at 125 μM concentration. Error is S.D. (C) Derivatization of the 6- and 7-positions of AQZ06 yielded compound **1**, which shows selective inhibition of F182A-mutant, but not wild-type, DDX3<sup>132-607</sup> in an ATPase assay. Error is S.D. (D,E) RNA duplex unwinding rates are identical for wild-type and F182A DDX3 when treated with compound **1**. Note that DDX3 is substoichiometric in the ATPase assays (B,C) but superstoichiometric in the duplex unwinding assays (D,E).

negative charges at these positions (data not shown), we did not find a substitution that dramatically increased potency. Our most potent compound (**1**) shows a biochemical IC<sub>50</sub> of ~100 μM in an ATPase assay [Fig. 7(C)]. However, we did not observe inhibition of duplex unwinding by compound **1** [Fig. 7(D,E)], which may be because DDX3 is superstoichiometric to RNA in this assay while substoichiometric in the ATPase assay. We did not test AQZ06 or compound **1** against Ded1p in yeast because the low on-target potency of these compounds suggest they may cause off-target effects like GXJ1-76, and anilinoquinazoline derivatives are pumped from

yeast by efflux pumps<sup>43</sup> (K.M.S. unpublished observations). Thus, we used chemical derivatization to increase the potency of AQZ01 against the F182A mutant of DDX3 greater than 10-fold while maintaining selectivity against wild-type DDX3.

## Discussion

We have demonstrated a strategy for analog sensitive inhibition of the DEAD-box protein DDX3. By generating expanded active-site mutations (Figs. 1 and 2) we sensitized DDX3 to inhibition by bulky kinase inhibitors (Fig. 4). Furthermore, treatment with the analog sensitive inhibitor GXJ1-76 is

sufficient to block yeast growth when yeast contain the expanded active-site allele F144A, however a *MCM3* mutant strain (*mcm3-1*) is also inhibited by this compound suggesting the effect may be due to off-target interactions (Fig. 5). We then found that anilinoquinazolines show selective biochemical inhibition of DDX3 F182A (Fig. 6) and made a series of derivatives to generate compound **1**, which selectively inhibits the mutant enzyme while sparing the wild-type (Fig. 7).

We targeted a hydrophobic cluster adjacent to the ATP binding site for mutation to generate the expanded active-site alleles. This region is broadly conserved in DEAD-box proteins in humans and other organisms [Fig. 1(B,C)], suggesting it may be possible to apply this strategy to other DEAD-box proteins besides DDX3. Our data on DDX3 already suggests a promising strategy to probe DDX3 function. However, prior to use in cells the affinity of the compound needs to be improved to avoid nonspecific toxicity (Fig. 5).

While using a kinase inhibitor scaffold as the starting point for our analog-sensitive DEAD-box helicase inhibitor immediately presents the problem of off-target toxicity towards cellular kinases, all the bulky inhibitors tested are remarkably inactive against most wild-type kinases. We hoped that by changing inhibitor scaffolds from the very promiscuous pyrazolopyrimidine to the more selective anilinoquinazoline we would additionally reduce this off-target toxicity. However, anilinoquinazolines have poor solubility and pharmacokinetic properties. Future work optimizing the scaffold with these considerations in mind could yield viable analog sensitive inhibitors of DDX3.

An additional challenge is the low potency of all tested chemical scaffolds for DDX3. While initial work generating an analog-sensitive kinase inhibitor used PP1, a nanomolar inhibitor of Src, as a starting point,<sup>44</sup> simple pyrazolopyrimidines and anilinoquinazolines are millimolar binders of DDX3. This is likely due to the fact that kinase inhibitors rely heavily on 'hinge' hydrogen bonding interactions for potency, and these contacts are not present in DEAD-box proteins. Making favorable interactions with the essential glutamine of the DEAD-box helicase Q-motif could provide a substantial jump in potency.<sup>45</sup> Finding substituents that interact favorably with the helicase P-loop could also produce a similar potency boost. Since the majority of the affinity of AMP for the helicase active site is derived from the phosphate and not the adenosine,<sup>32</sup> it is possible that potent P-loop binders will provide the most promising path forward. We expect that additional rational design of compounds described within this work, along with additional screening for more potent leads, is a promising path towards developing

a potent chemical inhibitor of DDX3 and DEAD-box proteins in general.

## Materials and Methods

### Multiple sequence alignments

Sequences for all DEAD-box proteins from *Homo sapiens*, *Escherichia coli*, and *Saccharomyces cerevisiae* were retrieved from the NCBI and were aligned using MUSCLE.<sup>46</sup> A separate MUSCLE alignment of only human DEAD-box proteins was used to generate Figure 1(B). Alignments were visualized using Jalview.<sup>47</sup>

### Recombinant protein purification

The codon optimized coding sequence for human *DDX3X* residues 132-607 fused to a 6xHis-MBP tag was expressed in *E. coli* BL21-Star cells. Induction was performed by addition of 1 mM IPTG for 18 hours at 16°C. Cell pellets were lysed by sonication, clarified by centrifugation at ~30,000 g, and purified by nickel chromatography including a 1M NaCl wash to remove bound nucleic acids. The His-MBP tag was cleaved using tobacco etch virus protease during dialysis into 200 mM NaCl, 10% glycerol, 20 mM HEPES pH 7, and 0.5 mM TCEP. The sample was then purified using heparin affinity chromatography, eluted at 400 mM NaCl, 10% glycerol, 20 mM HEPES pH 7, and 0.5 mM TCEP, and applied to a Superdex 75 gel filtration column equilibrated in 500 mM NaCl, 10% glycerol, 20 mM HEPES pH 7.5 and 0.5 mM TCEP. Fractions were then concentrated to roughly 30  $\mu$ M and supplemented with 20% glycerol and flash frozen in LN2.

### RNA duplex unwinding

Duplex unwinding assays were performed as described<sup>33</sup> with 2 mM ATP (Fig. 2), 0.1 mM ATP (Figs. 3 and 7) or 0.5 mM ATP (Fig. 4) and 1  $\mu$ M protein. The sequences of the RNA duplex strands are 5'-AGCACCGUAAAGACGC-3' and 5'-GCGUCUUUACGGUGCUUAAAAACAAAACAAAA-CAAAA-3', and the short RNA strand was 5' radiolabeled with <sup>32</sup>P. Unlabeled "chase" RNA was not included. For experiments with inhibitors, protein, RNA and inhibitor were pre-incubated in helicase reaction buffer for five minutes and the reaction was initiated with ATP. All inhibitors were stored in DMSO and DMSO concentrations were matched between all experiments, which never exceeded 5%.

### Coupled ATPase assays

Assays were performed using ADP-Quest (DiscoverX) according to manufacturer's instructions with 1  $\mu$ M enzyme, 10  $\mu$ M dsRNA and 100  $\mu$ M ATP-gold (DiscoverX) in 20 mM Tris pH 7.5, 200 mM NaCl, 1 mM MgCl<sub>2</sub>, and 0.01% Triton X-100. The

sequences of the RNA duplex strands are the same as those used in the duplex unwinding assay. All experimental results are reported as the average of three replicates with error bars representing the standard deviation of results, except for Figure 6, which was completed without replicates.

### Yeast Experiments

A strain of *S. cerevisiae* containing a deletion of the *DED1* locus complemented by a *URA3* marked plasmid harboring *DED1* was described previously.<sup>4</sup> Mutants were generated by site-directed mutagenesis in a plasmid containing *DED1* marked with *HIS3*, which was then transformed into yeast and counterselected using 5-fluoroorotic acid on His<sup>-</sup> complete synthetic media. All strains were verified by plasmid purification and dideoxy sequencing. Strains were grown using YPD media following verification. Growth experiments in Figures 2D and 5B are tenfold dilutions from OD ~1; continuous growth experiments in Figure 5 are by OD<sub>595</sub> measurement at 30°C in a Tecan Infinite F200 plate reader with 2 mm orbital shaking.

### Acknowledgments

The authors thank Angie Hilliker and the lab of Jasper Rine for help with the yeast experiments and for sharing yeast strains, and Yoon-Jae Cho, Ray Deshaies, Jerry Pelletier, Flora Rutaganira and Joe Kliegman for sharing reagents and for suggestions on inhibitors to screen. S.N.F. is a Howard Hughes Medical Institute fellow of the Helen Hay Whitney Foundation, and J.A.D. and K.M.S. are Investigators of the Howard Hughes Medical Institute. The authors declare no conflict of interest. Author contributions: Conceptualization, S.N.F., K.J.B., K.M.S., and J.A.D.; Methodology, S.N.F., K.J.B. and K.J.C.; Investigation, S.N.F., K.J.B. and K.J.C.; Writing – Original Draft, S.N.F., K.J.B., K.M.S., and J.A.D.; Funding Acquisition, S.N.F., J.A.D. and K.M.S.; Supervision, J.A.D. and K.M.S.

### References

- Linder P, Jankowsky E (2011) From unwinding to clamping - the DEAD box RNA helicase family. *Nat Rev Mol Cell Biol* 12:505–516.
- Rajkowitz L, Chen D, Stampfl S, Semrad K, Waldsich C, Mayer O, Jantsch MF, Konrat R, Blasi U, Schroeder R (2007) RNA chaperones, RNA annealers and RNA helicases. *RNA Biol* 4:118–130.
- Shih JW, Wang WT, Tsai TY, Kuo CY, Li HK, Wu Lee YH (2012) Critical roles of RNA helicase DDX3 and its interactions with eIF4E/PABP1 in stress granule assembly and stress response. *Biochem J* 441:119–129.
- Hilliker A, Gao Z, Jankowsky E, Parker R (2011) The DEAD-box protein Ded1 modulates translation by the formation and resolution of an eIF4F-mRNA complex. *Mol Cell* 43:962–972.
- Brangwynne CP (2013) Phase transitions and size scaling of membrane-less organelles. *J Cell Biol* 203:875–881.
- Li P, Banjade S, Cheng HC, Kim S, Chen B, Guo L, Llaguno M, Hollingsworth JV, King DS, Banani SF, Russo PS, Jiang QX, Nixon BT, Rosen MK (2012) Phase transitions in the assembly of multivalent signalling proteins. *Nature* 483:336–340.
- Kato M, Han TW, Xie S, Shi K, Du X, Wu LC, Mirzaei H, Goldsmith EJ, Longgood J, Pei J, Grishin NV, Frantz DE, Schneider JW, Chen S, Li L, Sawaya MR, Eisenberg D, Tycko R, McKnight SL (2012) Cell-free formation of RNA granules: low complexity sequence domains form dynamic fibers within hydrogels. *Cell* 149:753–767.
- Hubstenberger A, Noble SL, Cameron C, Evans TC (2013) Translation repressors, an RNA helicase, and developmental cues control RNP phase transitions during early development. *Dev Cell* 27:161–173.
- Lai MC, Chang WC, Shieh SY, Tarn WY (2010) DDX3 regulates cell growth through translational control of cyclin E1. *Mol Cell Biol* 30:5444–5453.
- Lee CS, Dias AP, Jedrychowski M, Patel AH, Hsu JL, Reed R (2008) Human DDX3 functions in translation and interacts with the translation initiation factor eIF3. *Nucleic Acids Res* 36:4708–4718.
- de la Cruz J, Iost I, Kressler D, Linder P (1997) The p20 and Ded1 proteins have antagonistic roles in eIF4E-dependent translation in *Saccharomyces cerevisiae*. *Proc Natl Acad Sci USA* 94:5201–5206.
- Sen ND, Zhou F, Ingolia NT, Hinnebusch AG (2015) Genome-wide analysis of translational efficiency reveals distinct but overlapping functions of yeast DEAD-box RNA helicases Ded1 and eIF4A. *Genome Res* 25:1196–1205.
- Chuang RY, Weaver PL, Liu Z, Chang TH (1997) Requirement of the DEAD-Box protein ded1p for messenger RNA translation. *Science* 275:1468–1471.
- Jones DT, Jager N, Kool M, Zichner T, Hutter B, Sultan M, Cho YJ, Pugh TJ, Hovestadt V, Stutz AM, Rausch T, Warnatz HJ, Ryzhova M, Bender S, Sturm D, Pleier S, Cin H, Pfaff E, Sieber L, Wittmann A, Remke M, Witt H, Hutter S, Tzaridis T, Weischenfeldt J, Raeder B, Avci M, Amstislavskiy V, Zapatka M, Weber UD, Wang Q, Lasitschka B, Bartholomae CC, Schmidt M, von Kalle C, Ast V, Lawrenz C, Eils J, Kabbe R, Benes V, van Sluis P, Koster J, Volckmann R, Shih D, Betts MJ, Russell RB, Coco S, Tonini GP, Schuller U, Hans V, Graf N, Kim YJ, Monoranu C, Roggendorf W, Unterberg A, Herold-Mende C, Milde T, Kulozik AE, von Deimling A, Witt O, Maass E, Rössler J, Ebinger M, Schuhmann MU, Fruhwald MC, Hasselblatt M, Jabado N, Rutkowski S, von Bueren AO, Williamson D, Clifford SC, McCabe MG, Collins VP, Wolf S, Wiemann S, Lehrner H, Brors B, Scheurlen W, Felsberg J, Reifemberger G, Northcott PA, Taylor MD, Meyerson M, Pomeroy SL, Yaspo ML, Korbel JO, Korshunov A, Eils R, Pfister SM, Lichter P (2012) Dissecting the genomic complexity underlying medulloblastoma. *Nature* 488:100–105.
- Kool M, Jones DT, Jager N, Northcott PA, Pugh TJ, Hovestadt V, Piro RM, Esparza LA, Markant SL, Remke M, Milde T, Bourdeaut F, Ryzhova M, Sturm D, Pfaff E, Stark S, Hutter S, Seker-Cin H, Johann P, Bender S, Schmidt C, Rausch T, Shih D, Reimand J, Sieber L, Wittmann A, Linke L, Witt H, Weber UD, Zapatka M, König R, Beroukhir R, Bergthold G, van Sluis P, Volckmann R, Koster J, Versteeg R, Schmidt S, Wolf S, Lawrenz C, Bartholomae CC, von Kalle C,

- Unterberg A, Herold-Mende C, Hofer S, Kulozik AE, von Deimling A, Scheurlen W, Felsberg J, Reifenberger G, Hasselblatt M, Crawford JR, Grant GA, Jabado N, Perry A, Cowdrey C, Croul S, Zadeh G, Korbel JO, Doz F, Delattre O, Bader GD, McCabe MG, Collins VP, Kieran MW, Cho YJ, Pomeroy SL, Witt O, Brors B, Taylor MD, Schuller U, Korshunov A, Eils R, Wechsler-Reya RJ, Lichter P, Pfister SM, Project IPT (2014) Genome sequencing of SHH medulloblastoma predicts genotype-related response to smoothened inhibition. *Cancer Cell* 25:393–405.
16. Pugh TJ, Weeraratne SD, Archer TC, Pomeranz Krummel DA, Auclair D, Bochicchio J, Carneiro MO, Carter SL, Cibulskis K, Erlich RL, Greulich H, Lawrence MS, Lennon NJ, McKenna A, Meldrim J, Ramos AH, Ross MG, Russ C, Shefler E, Sivachenko A, Sogoloff B, Stojanov P, Tamayo P, Mesirov JP, Amani V, Teider N, Sengupta S, Francois JP, Northcott PA, Taylor MD, Yu F, Crabtree GR, Kautzman AG, Gabriel SB, Getz G, Jager N, Jones DT, Lichter P, Pfister SM, Roberts TM, Meyerson M, Pomeroy SL, Cho YJ (2012) Medulloblastoma exome sequencing uncovers subtype-specific somatic mutations. *Nature* 488:106–110.
  17. Robinson G, Parker M, Kranenburg TA, Lu C, Chen X, Ding L, Phoenix TN, Hedlund E, Wei L, Zhu X, Chalhoub N, Baker SJ, Huether R, Kriwacki R, Curley N, Thiruvengadam R, Wang J, Wu G, Rusch M, Hong X, Becksfort J, Gupta P, Ma J, Easton J, Vadodaria B, Onar-Thomas A, Lin T, Li S, Pounds S, Paugh S, Zhao D, Kawauchi D, Roussel MF, Finkelstein D, Ellison DW, Lau CC, Bouffet E, Hassall T, Gururangan S, Cohn R, Fulton RS, Fulton LL, Dooling DJ, Ochoa K, Gajjar A, Mardis ER, Wilson RK, Downing JR, Zhang J, Gilbertson RJ (2012) Novel mutations target distinct subgroups of medulloblastoma. *Nature* 488:43–48.
  18. Jiang L, Gu ZH, Yan ZX, Zhao X, Xie YY, Zhang ZG, Pan CM, Hu Y, Cai CP, Dong Y, Huang JY, Wang L, Shen Y, Meng G, Zhou JF, Hu JD, Wang JF, Liu YH, Yang LH, Zhang F, Wang JM, Wang Z, Peng ZG, Chen FY, Sun ZM, Ding H, Shi JM, Hou J, Yan JS, Shi JY, Xu L, Li Y, Lu J, Zheng Z, Xue W, Zhao WL, Chen Z, Chen SJ (2015) Exome sequencing identifies somatic mutations of DDX3X in natural killer/T-cell lymphoma. *Nat Genet* 47:1061–1066.
  19. Ojha J, Secreto CR, Rabe KG, Van Dyke DL, Kortum KM, Slager SL, Shanafelt TD, Fonseca R, Kay NE, Braggio E (2015) Identification of recurrent truncated DDX3X mutations in chronic lymphocytic leukaemia. *Br J Haematol* 169:445–448.
  20. Schmitz R, Young RM, Ceribelli M, Jhavar S, Xiao W, Zhang M, Wright G, Shaffer AL, Hodson DJ, Buras E, Liu X, Powell J, Yang Y, Xu W, Zhao H, Kohlhammer H, Rosenwald A, Kluin P, Muller-Hermelink HK, Ott G, Gascoyne RD, Connors JM, Rimsza LM, Campo E, Jaffe ES, Delabie J, Smeland EB, Olgwang MD, Reynolds SJ, Fisher RI, Braziel RM, Tubbs RR, Cook JR, Weisenburger DD, Chan WC, Pittaluga S, Wilson W, Waldmann TA, Rowe M, Mbulaitaye SM, Rickinson AB, Staudt LM (2012) Burkitt lymphoma pathogenesis and therapeutic targets from structural and functional genomics. *Nature* 490:116–120.
  21. Wang L, Lawrence MS, Wan Y, Stojanov P, Sougnez C, Stevenson K, Werner L, Sivachenko A, DeLuca DS, Zhang L, Zhang W, Vartanov AR, Fernandes SM, Goldstein NR, Folco EG, Cibulskis K, Tesar B, Sievers QL, Shefler E, Gabriel S, Hacohen N, Reed R, Meyerson M, Golub TR, Lander ES, Neuberger D, Brown JR, Getz G, Wu CJ (2011) SF3B1 and other novel cancer genes in chronic lymphocytic leukemia. *N Engl J Med* 365:2497–2506.
  22. Seiwert TY, Zuo Z, Keck MK, Khattri A, Pedamallu CS, Stricker T, Brown C, Pugh TJ, Stojanov P, Cho J, Lawrence MS, Getz G, Bragelmann J, DeBoer R, Weichselbaum RR, Langerman A, Portugal L, Blair E, Stenson K, Lingen MW, Cohen EE, Vokes EE, White KP, Hammerman PS (2015) Integrative and comparative genomic analysis of HPV-positive and HPV-negative head and neck squamous cell carcinomas. *Clin Cancer Res* 21:632–641.
  23. Stransky N, Egloff AM, Tward AD, Kostic AD, Cibulskis K, Sivachenko A, Kryukov GV, Lawrence MS, Sougnez C, McKenna A, Shefler E, Ramos AH, Stojanov P, Carter SL, Voet D, Cortes ML, Auclair D, Berger MF, Saksena G, Guiducci C, Onofrio RC, Parkin M, Romkes M, Weissfeld JL, Seethala RR, Wang L, Rangel-Escareno C, Fernandez-Lopez JC, Hidalgo-Miranda A, Melendez-Zajgla J, Winckler W, Ardlie K, Gabriel SB, Meyerson M, Lander ES, Getz G, Golub TR, Garraway LA, Grandis JR (2011) The mutational landscape of head and neck squamous cell carcinoma. *Science* 333:1157–1160.
  24. Bol GM, Vesuna F, Xie M, Zeng J, Aziz K, Gandhi N, Levine A, Irving A, Korz D, Tantravedi S, Heerma van Voss MR, Gabrielson K, Bordt EA, Polster BM, Cope L, van der Groep P, Kondaskar A, Rudek MA, Hosmane RS, van der Wall E, van Diest PJ, Tran PT, Raman V (2015) Targeting DDX3 with a small molecule inhibitor for lung cancer therapy. *EMBO Mol Med* 7:648–669.
  25. Lorsch JR, Herschlag D (1998) The DEAD box protein eIF4A. 1. A minimal kinetic and thermodynamic framework reveals coupled binding of RNA and nucleotide. *Biochemistry* 37:2180–2193.
  26. Liu F, Putnam A, Jankowsky E (2008) ATP hydrolysis is required for DEAD-box protein recycling but not for duplex unwinding. *Proc Natl Acad Sci USA* 105:20209–20214.
  27. Lopez MS, Kliegman JI, Shokat KM (2014) The logic and design of analog-sensitive kinases and their small molecule inhibitors. *Methods Enzymol* 548:189–213.
  28. Hertz NT, Berthet A, Sos ML, Thorn KS, Burlingame AL, Nakamura K, Shokat KM (2013) A neo-substrate that amplifies catalytic activity of parkinson's-disease-related kinase PINK1. *Cell* 154:737–747.
  29. Gillespie PG, Gillespie SK, Mercer JA, Shah K, Shokat KM (1999) Engineering of the myosin- $\beta$  nucleotide-binding pocket to create selective sensitivity to N(6)-modified ADP analogs. *J Biol Chem* 274:31373–31381.
  30. Kapoor TM, Mitchison TJ (1999) Allele-specific activators and inhibitors for kinesin. *Proc Natl Acad Sci USA* 96:9106–9111.
  31. Floor SN, Condon KJ, Sharma D, Jankowsky E, Doudna JA (in press) Autoinhibitory interdomain interactions and subfamily-specific extensions redefine the catalytic core of the human DEAD-box protein DDX3. *J Biol Chem* 2015. DOI: 10.1074/jbc.M115.700625 [Epub ahead of print].
  32. Putnam AA, Jankowsky E (2013) AMP sensing by DEAD-box RNA helicases. *J Mol Biol* 425:3839–3845.
  33. Jankowsky E, Putnam A (2010) Duplex unwinding with DEAD-box proteins. *Methods Mol Biol* 587:245–264.
  34. Jamieson DJ, Beggs JD (1991) A suppressor of yeast spp81/ded1 mutations encodes a very similar putative ATP-dependent RNA helicase. *Mol Microbiol* 5:805–812.
  35. Maga G, Falchi F, Radi M, Botta L, Casaluce G, Bernardini M, Irannejad H, Manetti F, Garbelli A, Samuele A, Zanolli S, Este JA, Gonzalez E, Zucca E,

- Paolucci S, Baldanti F, De Rijck J, Debyser Z, Botta M (2011) Toward the discovery of novel anti-HIV drugs. Second-generation inhibitors of the cellular ATPase DDX3 with improved anti-HIV activity: synthesis, structure-activity relationship analysis, cytotoxicity studies, and target validation. *ChemMedChem* 6:1371–1389.
36. Samal SK, Routray S, Veeramachaneni GK, Dash R, Botlagunta M (2015) Ketorolac salt is a newly discovered DDX3 inhibitor to treat oral cancer. *Sci Rep* 5: 9982.
  37. Mathi P, Nikhil K, Ambatipudi N, Roy P, Bokka VR, Botlagunta M (2014) In-vitro and in-silico characterization of *Sophora interrupta* plant extract as an anti-cancer activity. *Bioinformation* 10:144–151.
  38. Yang Q, Jankowsky E (2005) ATP- and ADP-dependent modulation of RNA unwinding and strand annealing activities by the DEAD-box protein DED1. *Biochemistry* 44:13591–11601.
  39. Chou TF, Brown SJ, Minond D, Nordin BE, Li K, Jones AC, Chase P, Porubsky PR, Stoltz BM, Schoenen FJ, Patricelli MP, Hodder P, Rosen H, Deshaies RJ (2011) Reversible inhibitor of p97, DBeQ, impairs both ubiquitin-dependent and autophagic protein clearance pathways. *Proc Natl Acad Sci USA* 108:4834–4839.
  40. Bantscheff M, Eberhard D, Abraham Y, Bastuck S, Boesche M, Hobson S, Mathieson T, Perrin J, Raida M, Rau C, Reader V, Sweetman G, Bauer A, Bouwmeester T, Hopf C, Kruse U, Neubauer G, Ramsden N, Rick J, Kuster B, Drewes G (2007) Quantitative chemical proteomics reveals mechanisms of action of clinical ABL kinase inhibitors. *Nat Biotechnol* 25:1035–1044.
  41. Cencic R, Galicia-Vazquez G, Pelletier J (2012) Inhibitors of translation targeting eukaryotic translation initiation factor 4A. *Methods Enzymol* 511:437–461.
  42. Gibson SI, Surosky RT, Tye BK (1990) The phenotype of the minichromosome maintenance mutant *mcm3* is characteristic of mutants defective in DNA replication. *Mol Cell Biol* 10:5707–5720.
  43. Kung C, Kenski DM, Krukenberg K, Madhani HD, Shokat KM (2006) Selective kinase inhibition by exploiting differential pathway sensitivity. *Chem Biol* 13:399–407.
  44. Bishop AC, Shah K, Liu Y, Witucki L, Kung C, Shokat KM (1998) Design of allele-specific inhibitors to probe protein kinase signaling. *Curr Biol* 8:257–266.
  45. Tanner NK, Cordin O, Banroques J, Doere M, Linder P (2003) The Q motif: a newly identified motif in DEAD box helicases may regulate ATP binding and hydrolysis. *Mol Cell* 11:127–138.
  46. Edgar RC (2004) MUSCLE: multiple sequence alignment with high accuracy and high throughput. *Nucleic Acids Res* 32:1792–1797.
  47. Waterhouse AM, Procter JB, Martin DM, Clamp M, Barton GJ (2009) Jalview Version 2—a multiple sequence alignment editor and analysis workbench. *Bioinformatics* 25:1189–1191.